Unity-Bounded Function and Benchmark Design Specifications Targeted for Designing Typical Variable Digital Filters

Tian-Bo Deng(✉)

Department of Information Science, Faculty of Science, Toho University, Miyama 2-2-1, Funabashi, Chiba 274-8510, Japan
deng@is.sci.toho-u.ac.jp

Abstract. This paper first presents a set of benchmark design specifications that include variable lowpass specification, variable highpass specification, variable bandpass specification, variable bandstop specification, and variable notch specification. The design specifications are targeted for testing and verifying the effectiveness of various newly developed algorithms for designing typical variable digital filters. The paper then provides a novel unity-bounded function developed for guaranteeing the stability of a recursive variable transfer function. Finally, demonstrative results using one of the benchmark design specifications and the unity-bounded function are illustrated.

Keywords: Variable digital filter (VDF) · Benchmark specification · Typical filter · Unity-bounded function · Amplitude response · Recursive VDF · Stability

1 Introduction

Digital filters play extremely important roles in a vast number of fields such as signal processing, speech processing, image processing, automatic control, digital communications, and other information technology (IT) and artificial-intelligence (AI)-related fields. If the coefficients of a digital filter are fixed, the frequency-domain property of such a filter is also fixed. Indeed, many practical applications necessitate tunable frequency-domain responses (properties) during filtering process. The digital filter with frequency-response tunability is called variable digital filter (VDF). To tune the frequency response, one can parameterize the VDF coefficients as functions of the parameters that are used to tune the frequency response. Through simply varying the values of VDF coefficients, one can update the frequency response. In other words, a VDF has the coefficients that are usually the functions of the parameters that are used to vary the frequency response. As an example, a parameter may be used to tune the bandwidths of a VDF. For simplicity, this paper only discusses the simplest case with only a single parameter.

A VDF may have variable fractional delay [1–8], and such a VDF has unity amplitude. This paper deals with the VDFs that have tunable amplitude responses [9–15], and

Y. Kambayashi et al. (Eds.): AICON 2022, LNICST 477, pp. 107–120, 2023.
https://doi.org/10.1007/978-3-031-29126-5_9

summarizes two major contributions. The first key point is to present a set of typical benchmark design specifications (amplitude specifications) that are spefically developed for VDF designs. Those benchmark design specifications include variable lowpass specification, variable highpass specification, variable bandpass specification, variable bandstop specification, and variable notch-frequency specification. Such typical design specifications are targeted for the design of various typical VDFs, including variable lowpass filter, variable highpass filter, variable bandpass filter, variable bandstop filter, and variable notch-frequency filter. In other words, the major objective of this paper is to present those basic design specifications such that the filter designer can take any of them as a benchmark design specification for testing and verifying the effectiveness of various developed VDF design algorithms. This paper also aims to present a new function called unity-bounded function, which can be employed in guaranteeing the stability of recursive VDFs [10, 15]. Employing the unity-bounded function ensures that the filter designer is able to get a recursive VDF with guaranteed stability. That is, the resulting transfer function is an absolutely stabilized mathematical model for a recursive VDF. Finally, both the presented benchmark design specifications and the new unity bounded function is used to design recursive digital filters with various bandwidths. The computer simulation results verify that the developed unity-bounded function is useful in getting high-performance recursive digital filters with variable bandwidths. Furthermore, the designed recursive digital filters with different bandwidths are stable.

2 Typical Benchmark Specifications

A recursive VDF can be described by using the mathematical model (transfer function)

$$H(z,\rho) = \frac{\sum\limits_{k=0}^{N} a_k(\rho) z^{-k}}{\prod\limits_{k=1}^{N/2} \left[1 + b_{k,1}(\rho) z^{-k} + b_{k,2}(\rho) z^{-2}\right]}. \tag{1}$$

As long as a VDF that has variable amplitude response is concerned, its frequency bandwidths are variable. In (1), ρ is a parameter utilized for changing the bandwidths of $H(z, \rho)$, and the coefficients of $H(z, \rho)$ are not constant, but the functions of ρ. For simplicity, the parameter ρ is called the bandwith (BW)-tuning parameter. Although we discuss only one parameter ρ in this paper, the idea in this paper can be readily generalized to the case where a VDF has the coefficients parameterized as the functions of multi-parameters.

As mentioned above, all the coefficients $a_k(\rho)$, $b_{k,1}(\rho)$, and $b_{k,2}(\rho)$ are the functions of the BW-tuning parameter ρ. Once $a_k(\rho)$, $b_{k,1}(\rho)$, and $b_{k,2}(\rho)$ are determined, one can change the values of ρ and thus get the new values of the coefficients $a_k(\rho)$, $b_{k,1}(\rho)$, $b_{k,2}(\rho)$, which leads to the changes of the bandwidths of $H(z, \rho)$.

Assume that the desired (ideal) amplitude response $A_{\mathrm{d}}(\omega, \rho)$ is given. The objective of designing a VDF is to determine the optimal functions $a_k(\rho)$, $b_{k,1}(\rho)$, and $b_{k,2}(\rho)$ in such a manner that the desired amplitude response $A_{\mathrm{d}}(\omega, \rho)$ is best approximated through minimizing a specifically defined error function. That is, the problem is about how to find the optimal functions $a_k(\rho)$, $b_{k,1}(\rho)$, and $b_{k,2}(\rho)$. The next subsection provides a set of typical amplitude design specifications that can be taken as benchmark specifications in designing various typical VDFs. The utilizations of those typical design specifications facilitate the VDF designers to evaluate various newly developed design techniques.

2.1 Variable Lowpass Design Specification

Let us consider the first design specification defined by

$$A_d(\omega, \rho) = \begin{cases} 1, \ \omega \in [0, \omega_\mathrm{p}] \\ 0, \ \omega \in [\omega_\mathrm{s}, \pi] \end{cases} \tag{2}$$

where the normalized radian frequency is ω [0, π], and ω_p and ω_s denote the passband-edge frequency and stopband-edge frequency, respectively,

$$\omega_\mathrm{p} = 0.30\pi + \rho$$
$$\omega_\mathrm{s} = 0.40\pi + \rho.$$

It is clear that this design specification is a variable lowpass amplitude, and both ω_p and ω_s can be tuned by using the single BW-tuning parameter

$$\rho \in [-0.10\pi, 0.10\pi].$$

This lowpass design specification is illustrated in Fig. 1, where both the passband width and the stopband width are variable, but the transition bandwidth is not variable (fixed at 0.10π).

2.2 Variable Highpass Design Specification

Next, let us consider the highpass design specification defined by

$$A_d(\omega, \rho) = \begin{cases} 0, \ \omega \in [0, \omega_\mathrm{s}] \\ 1, \ \omega \in [\omega_\mathrm{p}, \pi] \end{cases} \tag{3}$$

where ω_s and ω_p are stopband-edge frequency and passband-edge frequency, respectively,

$$\omega_\mathrm{s} = 0.60\pi + \rho$$
$$\omega_\mathrm{p} = 0.70\pi + \rho.$$

Similar to the above lowpass design specification, both ω_s and ω_p can be varied via changing the value of the single BW-tuning parameter

$$\rho \in [-0.10\pi, 0.10\pi].$$

Figure 2 shows the variable highpass amplitude specification, where the BW-tuning parameter ρ tunes passband width and stopband width, while the transition bandwidth remains fixed (0.10π).

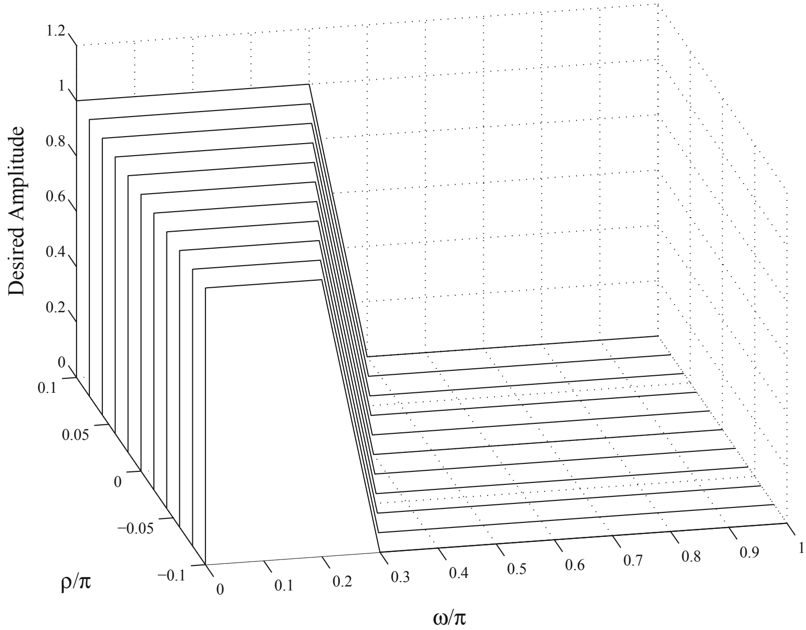

Fig. 1. Variable lowpass design specification

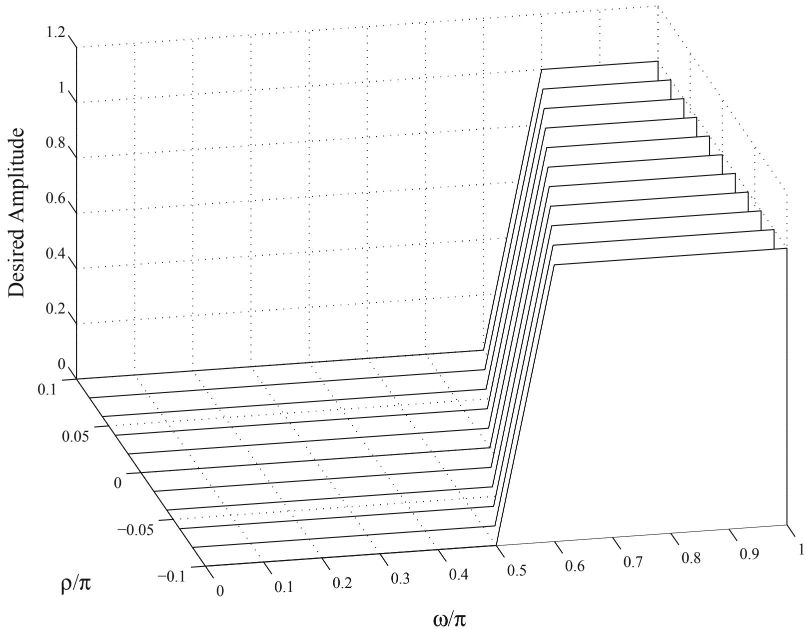

Fig. 2. Variable highpass design specification

2.3 Variable Bandpass Design Specification

The third one is the bandpass amplitude design specification defined by

$$A_s(\omega,\rho) = \begin{cases} 0, \ \omega \in [0, \omega_{\mathrm{s1}}] \\ 1, \ \omega \in \left[\omega_{\mathrm{p1}}, \omega_{\mathrm{p2}}\right] \\ 0, \ \omega \in [\omega_2, \pi] \end{cases} \tag{4}$$

where ω_{p1} and ω_{p2} denote two passband-edge frequencies, and ω_{s1}, ω_{s2} specify two stopband-edge frequencies. Those band-edge frequencies are defined by

$$\begin{aligned} \omega_{s1} &= 0.25\pi + \rho \\ \omega_{p1} &= 0.35\pi + \rho \\ \omega_{p2} &= 0.65\pi - \rho \\ \omega_{s2} &= 0.75\pi - \rho \end{aligned}$$

and the BW-tuning parameter is

$$\rho \in [-0.10\pi, 0.10\pi].$$

Figure 3 shows this variable bandpass design specification. Here, the two transition band- widths are also fixed (0.10π), while the passband width and stopband widths can be tuned through changing the value of parameter ρ.

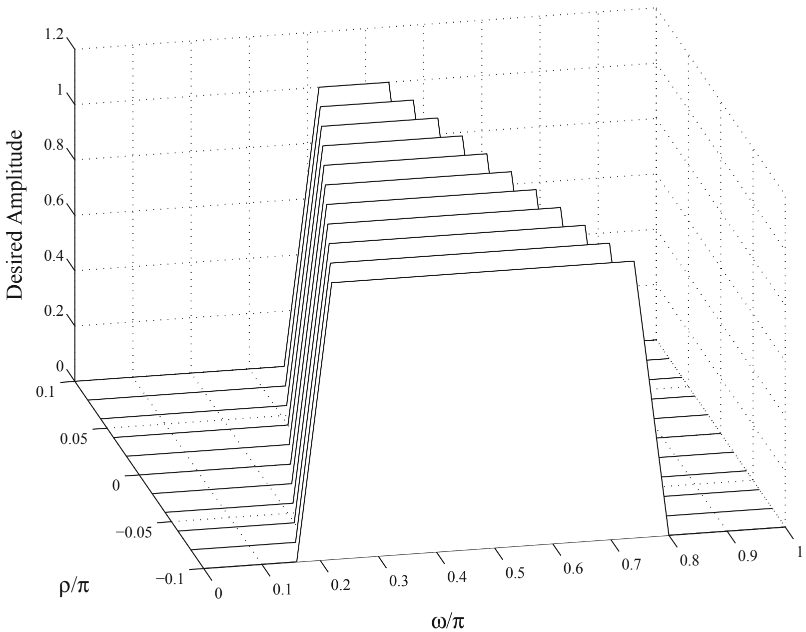

Fig. 3. Variable bandpass design specification

2.4 Variable Bandstop Design Specification

The next one is the bandstop design specification defined by

$$A_{\mathrm{d}}(\omega, \rho) = \begin{cases} 0, \ \omega \in \left[0, \omega_{\mathrm{p1}}\right] \\ 1, \ \omega \in [\omega_{\mathrm{s1}}, \omega_{\mathrm{s2}}] \\ 0, \ \omega \in \left[\omega_{\mathrm{p2}}, \pi\right] \end{cases} \tag{5}$$

where ω_{p1}, ω_{p2} denote two passband-edge frequencies, and ω_{s1}, ω_{s2} denote two stopband- edge frequencies. Those band-edge frequencies are defined by

$$\begin{aligned} \omega_{p1} &= 0.25\pi + \rho \\ \omega_{s1} &= 0.35\pi + \rho \\ \omega_{s2} &= 0.65\pi - \rho \\ \omega_{p2} &= 0.75\pi - \rho. \end{aligned}$$

Similarly, the above band-edge frequencies are tuned by

$$\rho \in [-0.10\pi, \ 0.10\pi].$$

Figure 4 illustrates this variable bandstop design specification, where the two passband widths and one stopband width are tuned by using ρ, while the two transition bandwidths keep constant (0.10π).

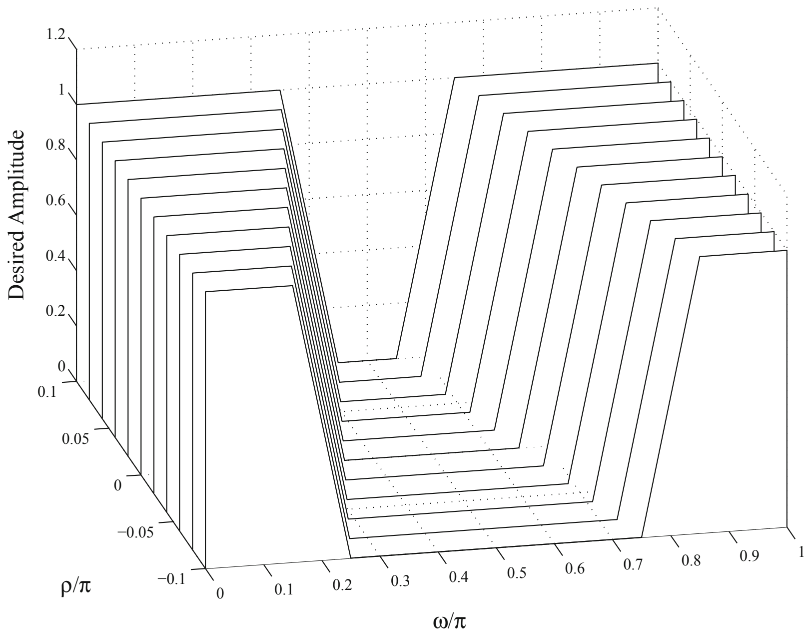

Fig. 4. Variable bandstop design specification

2.5 Variable Notch-Frequency Design Specification

Finally, let us consider the variable notch-frequency design specification defined by

$$A_{\mathrm{d}}(\omega, \rho) = \begin{cases} 0, \ \omega \in \left[0, \omega_{\mathrm{p1}}\right] \\ 1, \ \omega = \omega_{\mathrm{s}} \\ 0, \ \omega \in \left[\omega_{\mathrm{p2}}, \pi\right] \end{cases} \tag{6}$$

where $\omega_{\mathrm{p1}}, \omega_{\mathrm{p2}}$ are two passband-edge frequencies, and ω_{s} is the notch frequency. The band-edge frequencies are defined by

$$\begin{aligned} \omega_{p1} &= 0.40\pi + \rho \\ \omega_{s} &= 0.50\pi + \rho \\ \omega_{p2} &= 0.60\pi + \rho \end{aligned}$$

with

$$\rho \in [-0.10\pi, 0.10\pi].$$

Figure 5 shows this variable notch-frequency design specification. The notch frequency can be tuned by using the notch-tuning parameter ρ, while the two transition bandwidths are fixed at 0.10π.

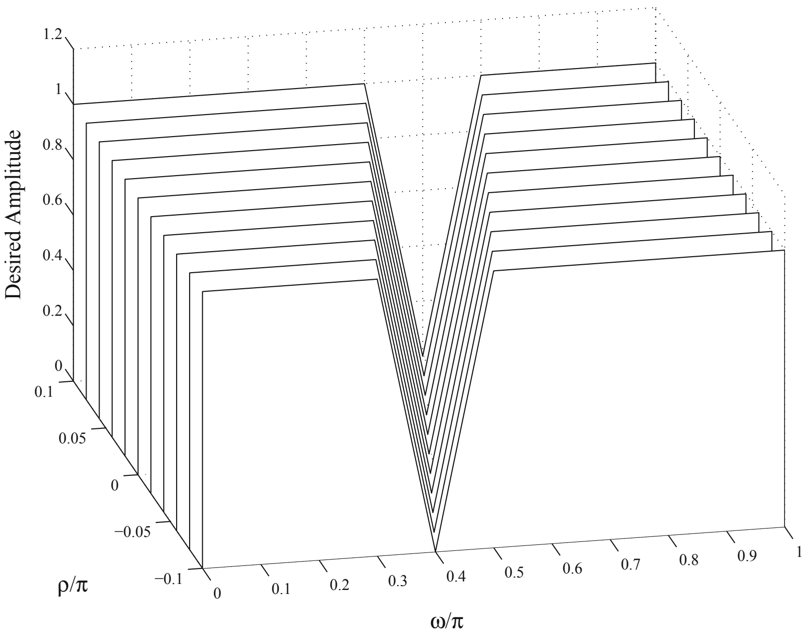

Fig. 5. Variable notch-frequency design specification

3 Unity-Bounded Function

The recursive VDF in (1) is stable if and only if the stability condition

$$\begin{cases} \left| b_{k,2}(\rho) < 1 \right| \\ \left| b_{k,1}(\rho) < 1 + b_{k,2}(\rho) \right| \end{cases} \tag{7}$$

is satisfied. Obviously, only the denominator coefficients $b_{k,2}(\rho)$, $b_{k,1}(\rho)$ determine whether or not the recursive VDF is stable. To guarantee the stability, an effective way is to transform denominator coefficients $b_{k,2}(\rho)$, $b_{k,1}(\rho)$ into the form

$$\begin{cases} b_{k,2}(\rho) = \beta \cdot U\big(x_{k,2}(\rho)\big) \\ b_{k,1}(\rho) = \beta \cdot U\big(x_{k,1}(\rho)\big)\big(1 + b_{k,2}(\rho)\big) \end{cases} \tag{8}$$

where

$$0 < \beta < 1$$

and $U(x)$ is a transformation function called unity-bounded function. The unity-bounded function exhibits the feature

$$U(x) \in [-1,\ 1] \tag{9}$$

and this condition is referred to as unity-bounded condition. One can rigorously (theoretically) prove that as long as $U(x)$ meets this unity-bounded condition, the stability, condition (7) is always met for arbitrary functions $x_{k,2}(\rho)$, $x_{k,1}(\rho)$. In designing a recursive VDF, the optimal functions $x_{k,2}(\rho)$, $x_{k,1}(\rho)$ need to be found, and they are usually assumed to be the polynomials in the parameter ρ. Here, a new unity-bounded function

$$U_x = \begin{cases} x, & |x| \le 1 \\ \mathrm{sign}(x), & |x| > 1 \end{cases} \tag{10}$$

is developed, where the sign function $\mathrm{sign}(x)$ is defined as

$$\mathrm{sign}(x) = \begin{cases} 1, & x > 0 \\ 0, & x = 0 \\ -1, & x < 0 \end{cases} \tag{11}$$

This unity-bounded function is illustrated in Fig. 6. Clearly, it satisfies the unity-bounded condition specified in (9).

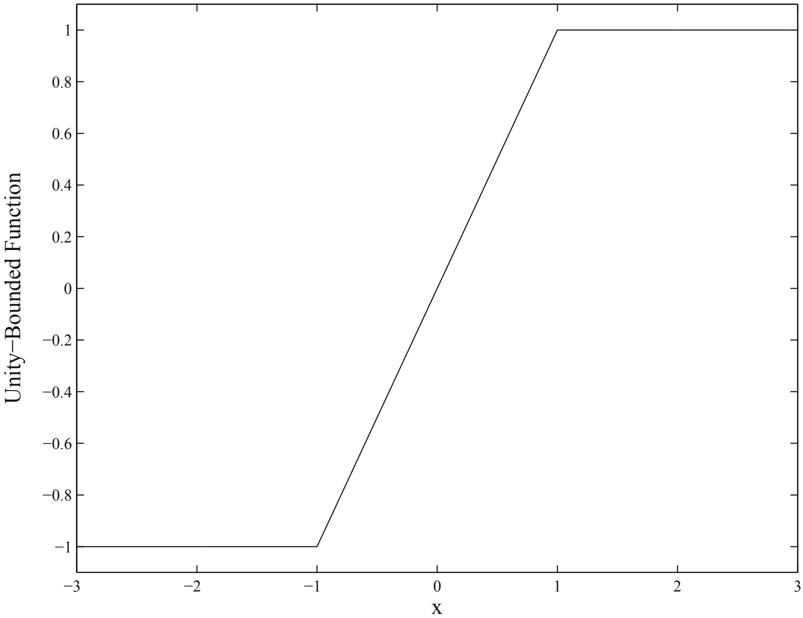

Fig. 6. Unity-bounded function $U(x)$

4 An Illustrative Example

In this section, the proposed unity-bounded function $U(x)$ in Fig. 6 is employed in designing a set of recursive digital filters for approximating the discretized notch specifications shown in Fig. 5, where each curve represents a discretized design specification associated with a sampled value of ρ. Although the variable notch specification in (6) is continuously tunable, this paper only deals with the approximations of the discretized notch specifications in Fig. 5, where the parameter ρ takes discretized values ρ_i, $i = 1$, 2, , I, and $I = 11$. Each curve in Fig. 5 represents a design specification with a different notch-frequency, and each of them is separately approximated by using an individual transfer function

$$H(z) = \frac{\sum_{k=0}^{N} a_k z^{-k}}{\prod_{k=1}^{N/2} \left[1 + b_{k,1} z^{-1} + b_{k,2} z^{-2}\right]}. \tag{12}$$

To ensure that the resulting recursive filters are stable, the unity-bounded function $U(x)$ is utilized to express the coefficients $b_{k,2}$, $b_{k,1}$ as the functions of $x_{k,2}$, $x_{k,1}$ as

$$\begin{cases} b_{k,2} = \beta \cdot U(x_k, 2) \\ b_{k,1} = \beta \cdot U\left(x_{k,1}\right)\left(1 + b_{k,2}\right). \end{cases} \tag{13}$$

Based on the above parameter transformations, the unknowns a_k, $x_{k,2}$, $x_{k,1}$ are optimized via employing a nonlinear programming. The design begins with the first filter corresponding to the first sample of ρ ($\rho_1 = -0.10\pi$), and sets the design parameters

$$\begin{aligned} &N = 8 \quad (\text{order of H}(z)) \\ &\beta = 0.99999 \quad (\text{factor small than untity}) \\ &I = 11 \quad (\text{number of samples } \rho_i) \\ &M = 201 \quad (\text{number of frequency samples } \omega_m) \\ &\left[a_k \; x_{k,2} \; z_{k,1}\right] = [0\,0 \cdots 0] \quad (\text{inital values}). \end{aligned}$$

As in [10–14], the design minimizes the weighted squared error of the amplitude response. Fig. 7 shows the desired amplitude (top), actual amplitude (middle), and design errors (bottom) of the first notch filter ($\rho_1 = -0.10\pi$), and Fig. 8 shows the stability triangles for this notch filter. Obviously, since all the four pairs ($b_{k,1}$, $b_{k,2}$) are located inside the stability triangles, it is concluded that the stability condition (7) is met, and the designed notch digital filter is stable.

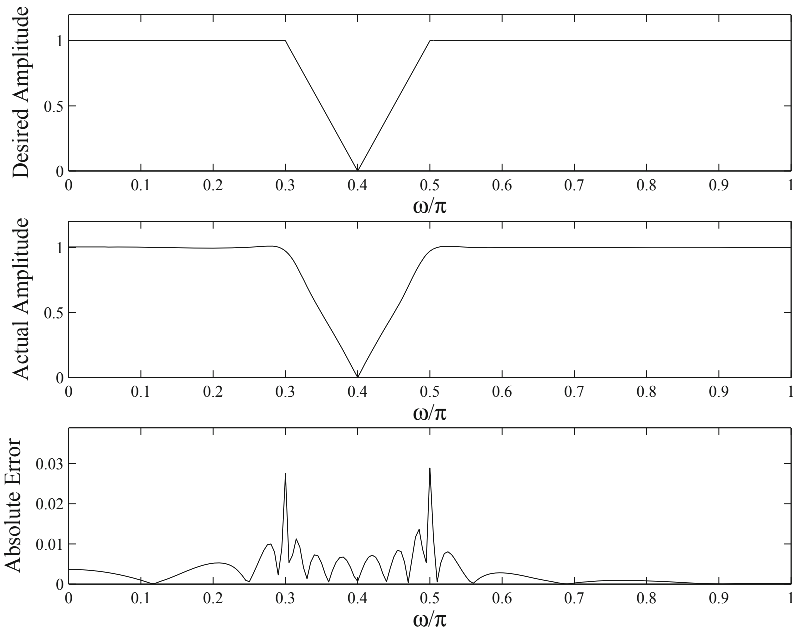

Fig. 7. Amplitude and errors of the notch filter ($\rho_1 = -0.10\pi$)

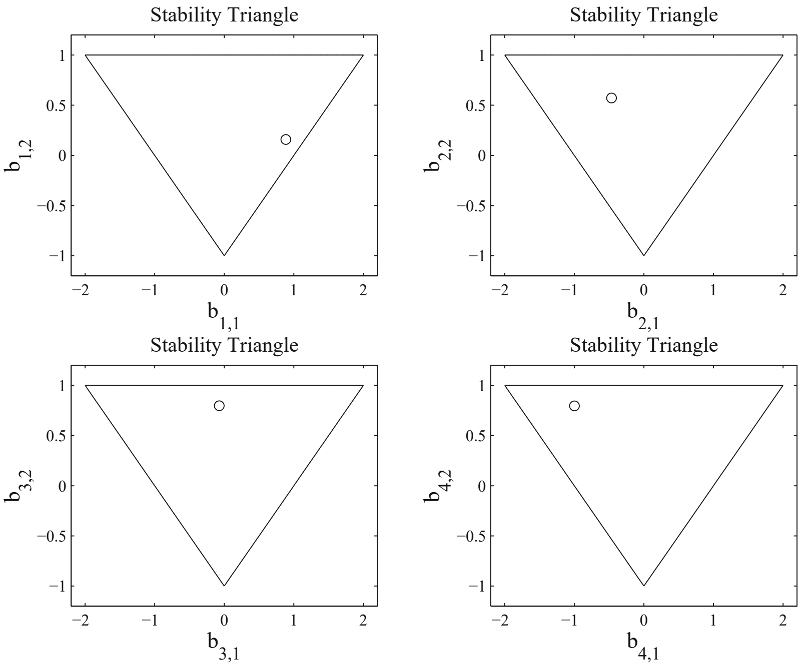

Fig. 8. Stability triangles for the notch filter ($\rho 1 = -0.10\pi$)

Next, let us check the last notch filter corresponding to $\rho_{11} = 0.10\pi$. Fig. 9 shows the desired amplitude (top), actual amplitude (middle), and design errors (bottom), and Fig. 10 shows the stability triangles. Similar to the first notch filter, all the pairs ($b_{k,1}$, $b_{k,2}$) are inside the stability triangles. Therefore, this recursive notch filter is also stable.

Finally, Fig. 11 plots the amplitude responses of all the notch filters ($I = 11$), and Fig. 12 plots the loci of the pairs ($b_{k,1}$, $b_{k,2}$) when ρ changes its value from ρ_1 to ρ_{11}. Again, Fig. 12 shows that all the pairs ($b_{k,1}$, $b_{k,2}$) are inside the stability triangles, which verifies that all the obtained notch filters are stable. The mean value of the normalized root-mean-squared (RMS) errors and the mean value of the maximum errors are

$$\overline{E}_2 = 0.5208\%, \ \overline{E}_{max} = 0.0315$$

respectively. The above simulation results indicate that the developed unity-bounded function for the parameter transformations not only can guarantee the stability, but also can produce VDFs with high accuracy.

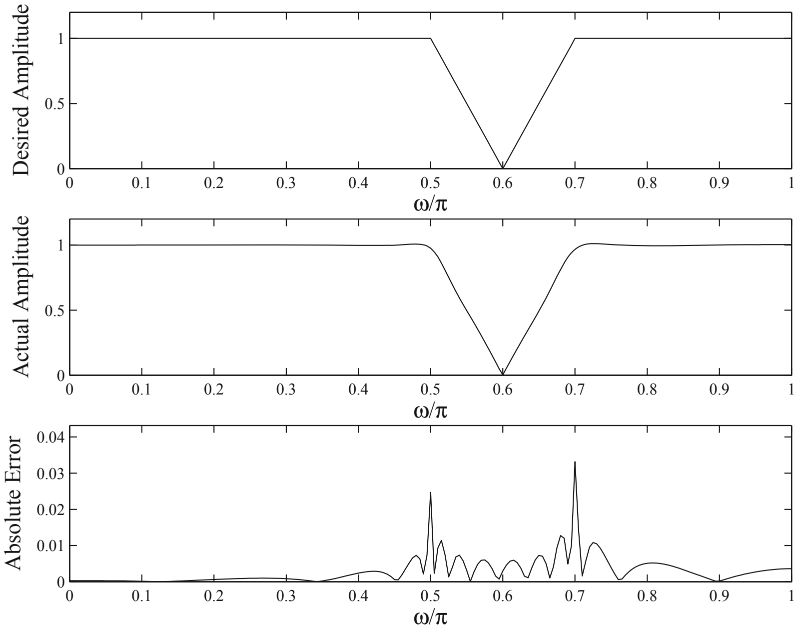

Fig. 9. Amplitude and errors of the last notch filter ($\rho_{11} = 0.10\pi$)

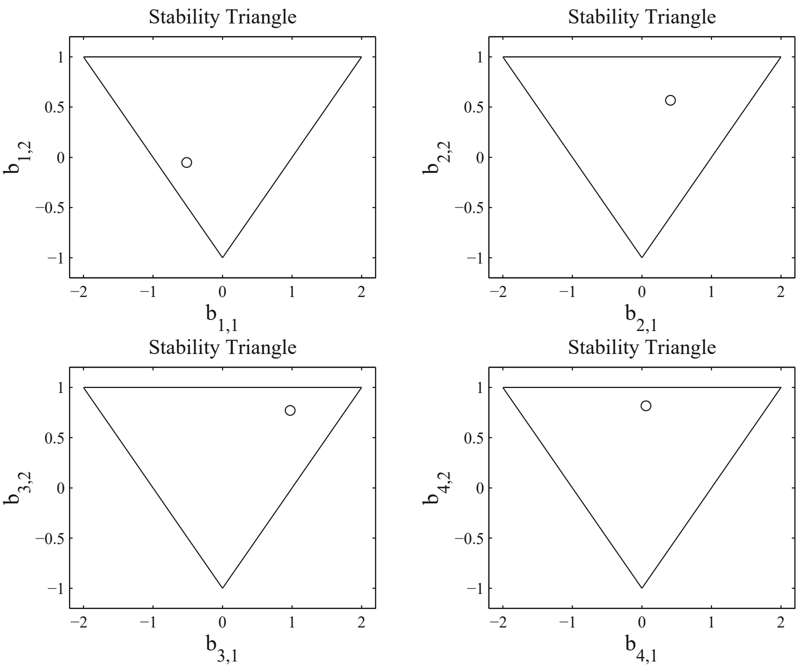

Fig. 10. Stability triangles for the last notch filter ($\rho 11 = 0.10\pi$)

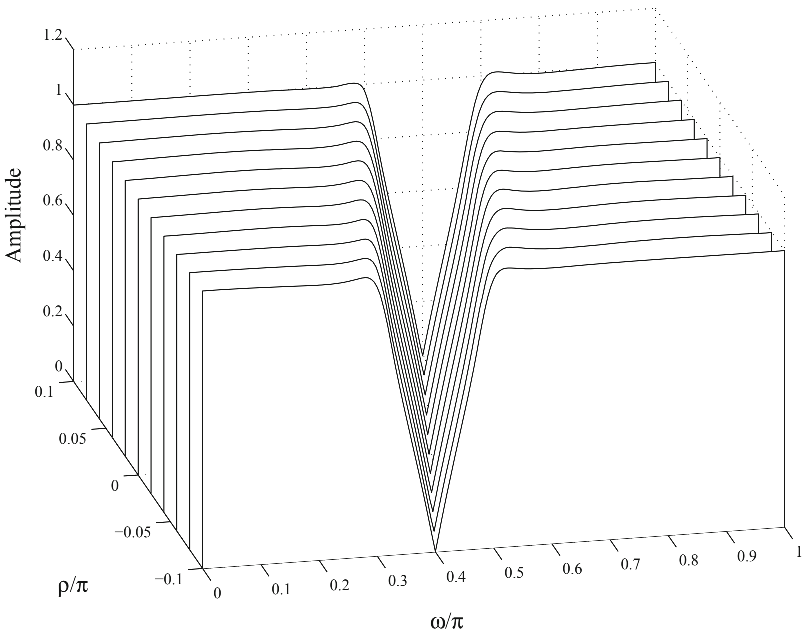

Fig. 11. Amplitude responses of all the notch filters ($I = 11$)

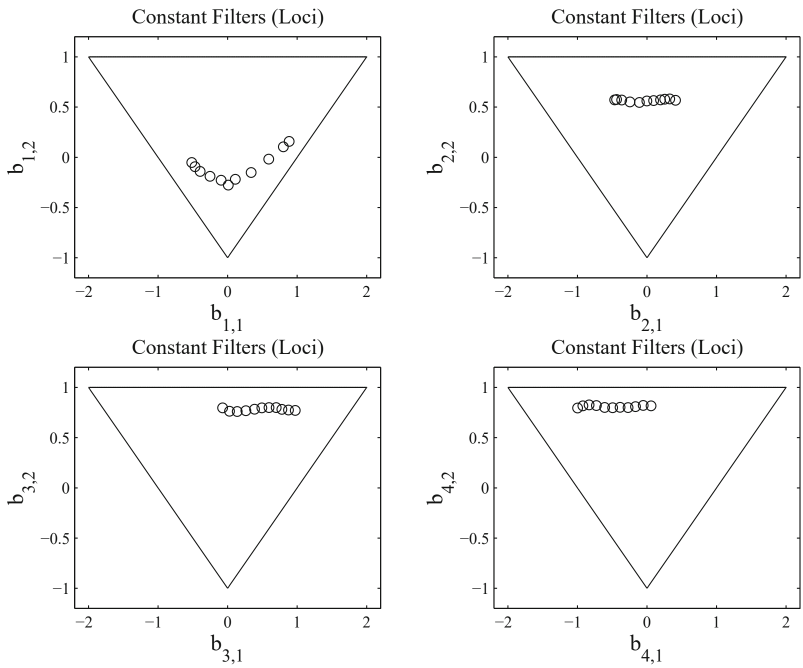

Fig. 12. Stability triangles for all the notch filters ($I = 11$)

5 Conclusion

This paper has presented a set of variable amplitude design specifications that can be taken as benchmark design specifications for designing typical VDFs, including variable lowpass VDF, variable highpass VDF, variable bandpass VDF, variable bandstop VDF, and variable notch VDF. Those typical design specifications can be used for evaluating and comparing various design algorithms in terms of design accuracy. Another major contribution of this paper is the development of the novel unity-bounded function required in guaranteeing the stability of recursive VDFs. The simulation results using the variable notch-frequency specification have verified that the newly developed unity-bounded function significantly facilitates the global search for excellent VDF coefficient values. Therefore, the developed unity-bounded function not only can guarantee the VDF stability, but also can produce considerably accurate VDFs.

References

1. Huang, Y.-D, Pei, S.-C., Shyu, J.-J.: WLS design of variable fractional-delay FIR filters using coefficient relationship. IEEE Trans. Circuits Syst. II, Exp. Briefs **56**(3), 220–224 (2009)
2. Deng, T.-B.: Discretization-free design of variable fractional-delay FIR digital filters. IEEE Trans. Circuits Syst. II, Analog Digit. Signal Process. **48**(6), 637–644 (2001)
3. Deng, T.-B., Nakagawa, Y.: SVD-based design and new structures for variable fractional-delay digital filters. IEEE Trans. Signal Process. **52**(9), 2513–2527 (2004)
4. Deng, T.-B., Lian, Y.: Weighted-least-squares design of variable fractional-delay FIR filters using coefficient-symmetry. IEEE Trans. Signal Process. **54**(8), 3023–3038 (2006)
5. Deng, T.-B.: Design and parallel implementation of FIR digital filters with simultaneously variable magnitude and non-integer phase-delay responses. IEEE Trans. Circuits Syst. II: Analog Digit. Signal Processing **50**(5), 243–250 (2003)
6. Deng, T.-B.: Closed-form design and efficient implementation of variable digital filters with simultaneously tunable magnitude and fractional-delay. IEEE Trans. Signal Process. **52**(6), 1668–1681 (2004)
7. Soontornwong, P., Chivapreecha, S.: Pascal-interpolation-based noninteger delay filter and low-complexity realization. Radioengineering **24**(4), 1002–1012 (2015)
8. Deng, T.-B.: Minimax design of low-complexity even-order variable fractional-delay filters using second-order cone programming. IEEE Trans. Circuits Syst. II: Express Briefs **58**(10), 692–696 (2011)
9. Zarour, R., Fahmy, M.M.: A design technique for variable digital filters. IEEE Trans. Circuits Syst. **36**(11), 1473–1478 (1989)
10. Deng, T.-B.: Design of recursive 1-D variable filters with guaranteed stability. IEEE Trans. Circuits Syst. II, Analog Digit. Signal Process. **44**(9), 689–695 (1997)
11. Deng, T.-B.: Design of variable 2-D linear phase recursive digital filters with guaranteed stability. IEEE Trans. Circuits Syst. I: Fundam. Theory Appl. **45**(8), 859–863 (1998)
12. Deng, T.-B.: Stability trapezoid and stability-margin analysis for the second-order recursive digital filter. Signal Process. **118**(1), 97–102 (2016)
13. Deng, T.-B.: Generalized stability-triangle for guaranteeing the stability-margin of the second-order digital filter. J. Circuits, Syst. Comput. **25**(8), 1650094 1–13 (2016)
14. Deng, T.-B.: Design of recursive variable-digital-filters with theoretically-guaranteed stability. Int. J. Electron. **103**(12), 2013–2028 (2016)
15. Deng, T.-B.: The Lp-norm-minimization design of stable variable-bandwidth digital filters. J. Circuits Syst. Comput. **27**(7), 1850102 1–18 (2018)